



Biofilm growth in a homogeneous porous medium
by Sunil Kumar Tiwari

A thesis submitted in partial fulfillment of the requirements for the degree of Doctor of Philosophy in
Mathematics

Montana State University

© Copyright by Sunil Kumar Tiwari (1997)

Abstract:

As biofilms intervene in a porous medium, they affect the porosity and permeability, which in turn alters the hydrodynamics. A biofilm growth model is presented which is suitable for microscale simulations of biofilm activity in a porous medium. The model is then used to predict the changing porosity and permeability. The predictions are compared to experimental data and finally these calculated properties are used to simulate flow in a biofilm infested porous medium.

BIOFILM GROWTH IN A HOMOGENEOUS POROUS MEDIUM

by

Sunil Kumar Tiwari

A thesis submitted in partial fulfillment
of the requirements for the degree

of

Doctor of Philosophy

in

Mathematics

MONTANA STATE UNIVERSITY
Bozeman, Montana

January 1997

D378
T5435

APPROVAL

of a thesis submitted by

Sunil Kumar Tiwari

This thesis has been read by each member of the thesis committee and has been found to be satisfactory regarding content, English usage, format, citations, bibliographic style, and consistency, and is ready for submission to the College of Graduate Studies.

1/17/97
Date

Kenneth L. Bowers
Kenneth L. Bowers
Chairperson, Graduate Committee

Approved for the Major Department

1/17/97
Date

John Lund
John Lund
Head, Mathematics

Approved for the College of Graduate Studies

1/23/97
Date

Robert Brown
Robert Brown
Graduate Dean

STATEMENT OF PERMISSION TO USE

In presenting this thesis in partial fulfillment for a doctoral degree at Montana State University, I agree that the Library shall make it available to borrowers under rules of the Library. I further agree that copying of this thesis is allowable only for scholarly purposes, consistent with "fair use" as prescribed in the U. S. Copyright Law. Requests for extensive copying or reproduction of this thesis should be referred to University Microfilms International, 300 North Zeeb Road, Ann Arbor, Michigan 48106, to whom I have granted "the exclusive right to reproduce and distribute copies of the dissertation for sale in and from microform or electronic format, along with the right to reproduce and distribute my abstract in any format in whole or in part."

Signature Sunil K. Jaisari

Date Jan 17' 1997

ACKNOWLEDGEMENTS

I am indebted to my advisor, Dr. Kenneth L. Bowers, for his guidance, support and encouragement throughout my association with him. In particular, his criticisms and suggestions during the writing of this thesis have been invaluable. My appreciation is also extended to professors Jack Dockery and Gary Bogar for their careful reading of this manuscript and their technical guidance.

I am grateful to Dr. Ken Tiahrt and Dr. John Lund for giving me the opportunity to continue my graduate studies at Montana State University. Thanks are also due to the rest of the faculty and my fellow graduate students who made my stay here such an enjoyable and intellectually rewarding experience. Special appreciation is due to the office staff of the Department of Mathematical Sciences who were very helpful.

Finally, I wish to thank my wife, Kala, for her patience, encouragement and support during these past years.

TABLE OF CONTENTS

	Page
LIST OF TABLES	viii
LIST OF FIGURES	xii
ABSTRACT	xviii
1. Introduction	1
2. Biofilm Models	6
Introduction	6
Rittman's Model	8
One-dimensional Model	8
Zero-dimensional Model	16
Biofilm Accumulation Model	19
One-dimensional Model	19
Zero-dimensional Model	25
Biofilm Growth Model	27
One-dimensional Model	27
Zero-dimensional Model	37
3. Comparison of the Biofilm Models	40
Introduction	40
Solution of One-dimensional BGM	41
Change in the Biofilm Thickness	44
Change in the Volume of the Bulk Liquid	44
Change in the Substrate Concentration in the Biofilm	45
Change in the Volume Fraction of the Active and Inactive Bacteria	46
Change in the Substrate Concentration in the Bulk Liquid	49
Comparison of Zero- and One-dimensional BGM	49
Change in the Biofilm Thickness	52
Change in the Volume of the Bulk Liquid	52
Change in Substrate Concentration in the Biofilm	53

Change in the Volume Fraction of Active and Inactive Bacteria	55
Change in the Substrate Concentration in the Bulk Liquid	58
Solution of Zero-dimensional Rittman's Model	63
Solution of Zero-dimensional BAM	69
Solution of Zero-dimensional BGM	77
Comparison of the Zero-dimensional Models	87
Substrate Concentration in the Bulk Liquid	87
Substrate Concentration in the Biofilm	90
Biofilm Thickness	90
Volume Fraction of Active Biomass	91
4. Biofilm Accumulation in Porous Media	92
Introduction	92
Flow of a Single Fluid Through Porous Media	93
Mass Balance and Momentum Balance	93
Incompressible Flow	95
Permeability and Porosity in Different Porous Media Models	98
Permeability in Bundles of Capillary Tubes Models	99
Permeability in Bed of Identical Spheres Models	103
Modelling Biofilm Accumulation in Porous Media	105
Biofilm Accumulation and Incompressible Fluid Flow	107
Biofilm Accumulation and One-dimensional Incompressible Flow	107
Biofilm Accumulation and Two-dimensional Incompressible Flow	110
5. Numerical Results	114
Introduction	114
Biofilm Growth in a Porous Medium	114
Algorithm	118
Biofilm Growth in a Short Bed	118
Validation of the Relation between Porosity and Permeability	119
Presentation of Numerical Results	122
Comparison of Numerical Results with Experimental Data	136
Another Verification	139
Prediction for a Long Bed Experiment	141
Conclusion	168
REFERENCES CITED	171
APPENDICES	174
APPENDIX A – Computer Code for Subroutine ODE23s	174
APPENDIX B – Computer Code for One-dimensional BGM	186
APPENDIX C – Computer Code for Zero-dimensional BGM-A	191

APPENDIX D - Computer Code for Zero-dimensional Rittman's Model .	194
APPENDIX E - Computer Code for Zero-dimensional BAM	197
APPENDIX F - Computer Code for One-dimensional BGM-B	200
APPENDIX G - Computer Code for Porous Media Flow and BGM . . .	203

LIST OF TABLES

Table		Page
1	Unknown dependent variables and their fundamental units in Rittman's one-dimensional model	9
2	Parameters and the variables used in Rittman's model and their fundamental units	10
3	Unknown dependent variables and their fundamental units in Rittman's zero-dimensional model	16
4	Parameters and the variables used in BAM and their fundamental units	20
5	Unknown dependent variables and their fundamental units in BAM zero-dimensional model	25
6	Unknown dependent variables and their fundamental units in the Biofilm Growth Model	28
7	Parameters and the variables used in Biofilm Growth Model and their fundamental units	29
8	Unknown dependent variables and their fundamental units in the zero-dimensional Biofilm Growth Model	37
9	Parameter values and initial values for one-dimensional BGM	43
10	Parameter values and initial values for the zero-dimensional BGM	51
11	Biofilm thickness, $L(t)$, over 50 days for the zero-dimensional and one-dimensional BGM	61
12	Volume, $V_L(t)$, of the bulk liquid over 50 days for zero-dimensional and one-dimensional BGM	62
13	Substrate concentration, $S(t)$, in the biofilm for the zero-dimensional BGM and the substrate concentration, $S(y, t)$, at points y_1 and y_2 in the biofilm for the one-dimensional BGM over 2 days	62
14	Substrate concentration, $S(t)$, in the biofilm for the zero-dimensional BGM and the substrate concentration, $S(y, t)$, at points y_1 and y_2 in the biofilm for the one-dimensional BGM over 50 days	63
15	Active biomass volume fraction, $f(t)$, for the zero-dimensional BGM and active biomass volume fraction, $f(y, t)$, at points y_1 and y_2 in the biofilm for the one-dimensional BGM over 35 days	64
16	Inactive biomass volume fraction, $\bar{f}(t)$, for the zero-dimensional BGM and inactive biomass volume fraction, $\bar{f}(y, t)$, at points y_1 and y_2 in the biofilm for the one-dimensional BGM over 35 days	65
17	The bulk substrate concentration, $S_b(t)$, for the zero-dimensional and one-dimensional BGM over .001 days	66

18	Parameter values and initial values for the zero-dimensional Rittman's model	68
19	Parameters values and the initial values for the zero-dimensional BAM	73
20	Parameter values and initial values for zero-dimensional BGM	78
21	Bulk substrate concentration, $S_b(t)$, over .001 days for the zero-dimensional Rittman's model (RIT), BAM, and BGM	81
22	Bulk substrate concentration, $S_b(t)$, over 10 days for the zero-dimensional Rittman's model (RIT), BAM, and BGM	81
23	Bulk substrate concentration, $S_b(t)$, over 50 days for the zero-dimensional Rittman's model (RIT), BAM, and BGM	82
24	Substrate concentrations, $S(t)$, in the film over .001 days for the zero-dimensional Rittman's model (RIT), BAM, and BGM	82
25	Substrate concentrations, $S(t)$, in the film over 10 days for the zero-dimensional Rittman's model (RIT), BAM, and BGM	83
26	Substrate concentrations, $S(t)$, in the film over 50 days for the zero-dimensional Rittman's model (RIT), BAM, and BGM	83
27	Biofilm thickness, $L(t)$, over .001 days for the zero-dimensional Rittman's model (RIT), BAM, and BGM	84
28	Biofilm thickness, $L(t)$, over 10 days for the zero-dimensional Rittman's model (RIT), BAM, and BGM	84
29	Biofilm thickness, $L(t)$, over 50 days for the zero-dimensional Rittman's model (RIT), BAM, and BGM	85
30	Active biomass volume fraction, $f(t)$, over .001 days for the zero-dimensional Rittman's model (RIT), BAM, and BGM	85
31	Active biomass volume fraction, $f(t)$, over 10 days for the zero-dimensional Rittman's model (RIT), BAM, and BGM	86
32	Active biomass volume fraction, $f(t)$, over 50 days for the zero-dimensional Rittman's model (RIT), BAM, and BGM	86
33	Unknown dependent variables in a porous media flow model and their fundamental units	94
34	Variables and constants used in the porous media flow model with their fundamental units	94
35	Variables and constants in bundles of capillary tubes models	100
36	Variables and constants in the bed of spherical particles model	105
37	Unknown dependent variables and their fundamental units in the one-dimensional incompressible fluid flow model with biofilm growth	117
38	Parameters and their fundamental units used in the one-dimensional incompressible porous media flow model with biofilm growth	117
39	The values of the parameters and the initial and boundary values of the unknown dependent variables used in the one-dimensional incompressible porous media flow model (short bed model) with biofilm growth and their units	120

40	Comparison of the normalized experimental permeability, $\hat{k}_e(z, t)$, the computed normalized permeabilities $\hat{k}_1(z, t)$ (using capillaric model) and $\hat{k}_2(z, t)$ (using the bed of spherical balls model) for the experimental porosity data from Cunningham's experimental model, [6].	122
41	Substrate concentration, $S_b(z, t)$, of the bulk liquid flowing through the pore channels of the porous medium over 20 days	124
42	Substrate concentration, $S(z, t)$, in the porous media biofilm on the spheres over 20 days	126
43	Active biomass volume fraction, $f(z, t)$, and inactive biomass volume fraction, $\bar{f}(z, t)$, over 20 days	128
44	Average biofilm thickness on the spheres, $L(z, t)$, over 20 days	130
45	Average pore volume, $V_L(z, t)$, over 20 days	131
46	Normalized numerical porosity, $\hat{\phi}_n(z, t)$, and normalized numerical permeability, $\hat{k}_n(z, t)$, over 20 days	134
47	Numerical volumetric flow rate, $Q_n(z, t)$, over 20 days	134
48	Normalized experimental porosity, $\hat{\phi}_e(z, t)$, and normalized numerical porosity, $\hat{\phi}_n(z, t)$, over 8 days	138
49	Normalized experimental permeability, $\hat{k}_e(z, t)$ and normalized numerical permeability, $\hat{k}_n(z, t)$, over 8 days	138
50	Experimental volumetric flow rate, $Q_e(z, t)$, and the numerical volumetric flow rate, $Q_n(z, t)$, over 8 days	140
51	Normalized experimental porosity, $\hat{\phi}_e(z, t)$, normalized numerical porosity, $\hat{\phi}_n(z, t)$, (using (5.14) and (5.15)), and the normalized numerical porosity, $\hat{\phi}_n^*(z, t)$, (using (5.16)) over 8 days	142
52	Normalized experimental permeability, $\hat{k}_e(z, t)$, normalized numerical permeability, $\hat{k}_n(z, t)$, (using (5.14) and (5.15)), and the normalized numerical permeability (using (5.16)), $\hat{k}_n^*(z, t)$, over 8 days	144
53	Experimental volumetric flow rate, $Q_e(z, t)$, the numerical volumetric flow rates, $Q_n(z, t)$, (using (5.14) and (5.15)), and $Q_n^*(z, t)$, (using (5.16)) over 8 days	144
54	The values of the parameters and the initial and boundary values of the unknown dependent variables used in the one-dimensional incompressible porous media flow model (long bed model) with biofilm growth and their units	146
55	Substrate concentration in the bulk liquid, $S_b(z, t)$, at the points z_1^* ($S_{b1}(t)$), z_2^* ($S_{b2}(t)$), and z_3^* ($S_{b3}(t)$) over 20 days.	148
56	Substrate concentration in the biofilm, $S(z, t)$, at the points z_1^* ($S_1(t)$), z_2^* ($S_2(t)$), and z_3^* ($S_3(t)$) over .001 days	149
57	Substrate concentration in the biofilm, $S(z, t)$, at the points z_1^* ($S_1(t)$), z_2^* ($S_2(t)$), and z_3^* ($S_3(t)$) over 1 day	150
58	Substrate concentration in the biofilm, $S(z, t)$, at the points z_1^* ($S_1(t)$), z_2^* ($S_2(t)$), and z_3^* ($S_3(t)$) over 20 days	151
59	Average active biomass volume fraction, $f(z, t)$, at the points z_1^* ($f_1(t)$), z_2^* ($f_2(t)$), and z_3^* ($f_3(t)$) over 1 day	154

60	Average active biomass volume fraction, $f(z, t)$, at the points $z_1^* (f_1(t))$, $z_2^* (f_2(t))$, and $z_3^* (f_3(t))$ over 20 days	154
61	Average inactive biomass volume fraction, $\bar{f}(z, t)$, at the points $z_1^* (\bar{f}_1(t))$, $z_2^* (\bar{f}_2(t))$, and $z_3^* (\bar{f}_3(t))$ over 1 day	155
62	Average inactive biomass volume fraction, $\bar{f}(z, t)$, at the points $z_1^* (\bar{f}_1(t))$, $z_2^* (\bar{f}_2(t))$, and $z_3^* (\bar{f}_3(t))$ over 20 days	155
63	Biofilm thickness $L(z, t)$, at the points $z_1^* (L_1(t))$, $z_2^* (L_2(t))$, and $z_3^* (L_3(t))$ over 5 days	157
64	Biofilm thickness $L(z, t)$, at the points $z_1^* (L_1(t))$, $z_2^* (L_2(t))$, and $z_3^* (L_3(t))$ over 20 days	157
65	Pore volume $V_L(z, t)$, at the points $z_1^* (V_{L1}(t))$, $z_2^* (V_{L2}(t))$, and $z_3^* (V_{L3}(t))$ over 5 days	159
66	Pore volume $V_L(z, t)$, at the points $z_1^* (V_{L1}(t))$, $z_2^* (V_{L2}(t))$, and $z_3^* (V_{L3}(t))$ over 20 days	159
67	Porosity $\phi(z, t)$, at the points $z_1^* (\phi_1(t))$, $z_2^* (\phi_2(t))$, and $z_3^* (\phi_3(t))$ over 5 days	161
68	Porosity $\phi(z, t)$, at the points $z_1^* (\phi_1(t))$, $z_2^* (\phi_2(t))$, and $z_3^* (\phi_3(t))$ over 20 days	162
69	Permeability $k(z, t)$, at the points $z_1^* (k_1(t))$, $z_2^* (k_2(t))$, and $z_3^* (k_3(t))$ over 5 days	163
70	Permeability $k(z, t)$, at the points $z_1^* (k_1(t))$, $z_2^* (k_2(t))$, and $z_3^* (k_3(t))$ over 20 days	164
71	Normalized porosity, $\hat{\phi}(z, t)$, at the points $z_1^* (\hat{\phi}_1(t))$, $z_2^* (\hat{\phi}_2(t))$, and $z_3^* (\hat{\phi}_3(t))$ over 20 days	165
72	Normalized permeability, $\hat{k}(z, t)$, at the points $z_1^* (\hat{k}_1(t))$, $z_2^* (\hat{k}_2(t))$, and $z_3^* (\hat{k}_3(t))$ over 20 days	165
73	Volumetric flow rate $Q(z, t)$, at the points $z_1^* (Q_1(t))$, $z_2^* (Q_2(t))$, and $z_3^* (Q_3(t))$ over 5 days	167
74	Volumetric flow rate $Q(z, t)$, at the points $z_1^* (Q_1(t))$, $z_2^* (Q_2(t))$, and $z_3^* (Q_3(t))$ over 20 days	168

LIST OF FIGURES

Figure		Page
1	Injection/recovery scheme for enhancing in situ bioremediation of contaminated aquifer. Inset shows the growing biofilm in porous media. .	2
2	Biofilm on a surface	7
3	Biofilm on a surface	11
4	Biofilm on a surface	20
5	Biofilm on a surface	28
6	Function $F(y)$ and the approximation of its integral over $[a, b]$	42
7	The thickness of the biofilm, $L(t)$, over 5 days (a) and 50 days (b) for the one-dimensional BGM	44
8	The volume of the bulk liquid, $V_L(t)$, over 5 days (a) and 50 days (b) for the one-dimensional BGM	45
9	The substrate concentration, $S(y, t)$, in the biofilm at points y_1 (dashed line) and y_2 (solid line) in the biofilm over 10^{-7} days (a), .0001 days (b), 2 days (c), and 15 days (d), for the one-dimensional BGM	47
10	The substrate concentration, $S(y, t)$, at points y_1 (dashed line) and y_2 (solid line) in the biofilm over 50 days for the one-dimensional BGM .	47
11	The active biomass volume fraction, $f(y, t)$, and the inactive biomass volume fraction, $\bar{f}(y, t)$, at points y_1 (dashed line) and y_2 (solid line) over 2.5 days for the one-dimensional BGM	48
12	The active biomass volume fraction, $f(y, t)$, and the inactive biomass volume fraction, $\bar{f}(y, t)$, at points y_1 (dashed line) and y_2 (solid line) over 50 days for the one-dimensional BGM	49
13	The substrate concentration, $S_b(t)$, in the bulk liquid over .001 days (a) and 50 days (b) for the one-dimensional BGM	50
14	Biofilm thickness, $L(t)$, over 5 days (a) and 50 days (b) for the zero-dimensional BGM	52
15	Biofilm thickness, $L(t)$, over 5 days (a) and 50 days (b) for the zero-dimensional (dash-dot line) and one-dimensional (solid line) BGM .	53
16	The bulk fluid volume, $V_L(t)$, over 5 days (a) and 50 days (b) for the zero-dimensional BGM	54
17	The bulk fluid volume, $V(t)$, over 5 (a) days and 50 days (b) for the zero-dimensional (dash-dot line) and one-dimensional (solid line) BGM	54
18	The substrate concentration, $S(t)$, over .0005 days for the zero-dimensional BGM	56
19	The substrate concentration, $S(t)$, over 2.5 days for the zero-dimensional BGM	56

20	The substrate concentration, $S(y, t)$, at points y_1 (dashed line) and y_2 (solid line) in the biofilm over 2.5 days for the one-dimensional BGM and the substrate concentration, $S(t)$, (dash-dot line) over 2.5 days for the zero-dimensional BGM	57
21	The substrate concentration, $S(t)$, over 50 days for the zero-dimensional BGM	57
22	The substrate concentration, $S(y, t)$, at points y_1 (dashed line) and y_2 (solid line) in the biofilm over 50 days for the one-dimensional BGM and the substrate concentration, $S(t)$, (dash-dot line) over 50 days for the zero-dimensional BGM	58
23	The active biomass volume fraction, $f(t)$, and inactive biomass volume fraction, $\bar{f}(t)$, over 2.5 days for the zero-dimensional BGM	59
24	The active biomass volume fraction, $f(t)$, and inactive biomass volume fraction, $\bar{f}(t)$, over 50 days for the zero-dimensional BGM	59
25	The active biomass volume fraction, $f(t)$, and inactive biomass volume fraction, $\bar{f}(t)$, over 5 days for the zero-dimensional BGM (dash-dot line) and the active biomass volume fraction, $f(y, t)$, and the inactive biomass volume fraction, $\bar{f}(y, t)$, at points y_1 (dashed line) and y_2 (solid line) over 5 days for the one-dimensional BGM	60
26	The active biomass volume fraction, $f(t)$, and inactive biomass volume fraction, $\bar{f}(t)$, over 50 days for the zero-dimensional BGM (dash-dot line) and the active biomass volume fraction, $f(y, t)$, and the inactive biomass volume fraction, $\bar{f}(y, t)$, at points y_1 (dashed line) and y_2 (solid line) over 50 days for the one-dimensional BGM	60
27	The substrate concentration, $S_b(t)$, in the bulk liquid, over .0005 days (a) and 50 days (b) for the zero-dimensional BGM	61
28	Bulk substrate concentration, $S_b(t)$ over .001 days, (a), and .05 days, (b) and substrate concentration in the biofilm, $S(t)$, over .001 days, (c), and .05 days, (d) for the zero-dimensional Rittman's model . . .	70
29	Bulk substrate concentration, $S_b(t)$, (a), biofilm thickness, $L(t)$, (b), substrate concentration in the biofilm, $S(t)$, (c), and active biomass volume fraction, $f(t)$, (d), over .001 days for the zero-dimensional Rittman's model	70
30	Bulk substrate concentration, $S_b(t)$, (a), biofilm thickness, $L(t)$, (b), substrate concentration in the biofilm, $S(t)$, (c), and active biomass volume fraction, $f(t)$, (d), over 10 days for the zero-dimensional Rittman's model	71
31	Bulk substrate concentration, $S_b(t)$, (a), biofilm thickness, $L(t)$, (b), substrate concentration in the biofilm, $S(t)$, (c), and active biomass volume fraction, $f(t)$, (d), over 50 days for the zero-dimensional Rittman's model	71
32	Bulk substrate concentration, $S_b(t)$ over .001 days, (a), and .05 days, (b) and substrate concentration in the biofilm, $S(t)$, over .001 days, (c), and .05 days, (d) for the zero-dimensional Rittman's model . . .	75

33	Bulk substrate concentration, $S_b(t)$, (a), biofilm thickness, $L(t)$, (b), substrate concentration in the biofilm, $S(t)$, (c), and active biomass volume fraction, $f(t)$, (d), over .001 days for the zero-dimensional BAM	75
34	Bulk substrate concentration, $S_b(t)$, (a), biofilm thickness, $L(t)$, (b), substrate concentration in the biofilm, $S(t)$, (c), and active biomass volume fraction, $f(t)$, (d), over 10 days for the zero-dimensional BAM	76
35	Bulk substrate concentration, $S_b(t)$, (a), biofilm thickness, $L(t)$, (b), substrate concentration in the biofilm, $S(t)$, (c), and active biomass volume fraction, $f(t)$, (d), over 50 days for the zero-dimensional BAM	76
36	Bulk substrate concentration, $S_b(t)$ over .001 days, (a), and .05 days, (b) and substrate concentration in the biofilm, $S(t)$, over .001 days, (c), and .05 days, (d) for the zero-dimensional BGM	79
37	Bulk substrate concentration, $S_b(t)$, (a), biofilm thickness, $L(t)$, (b), substrate concentration in the biofilm, $S(t)$, (c), and active biomass volume fraction, $f(t)$, (d), over .001 days for the zero-dimensional BGM	79
38	Bulk substrate concentration, $S_b(t)$, (a), biofilm thickness, $L(t)$, (b), substrate concentration in the biofilm, $S(t)$, (c), and active biomass volume fraction, $f(t)$, (d), over 10 days for the zero-dimensional BGM	80
39	Bulk substrate concentration, $S_b(t)$, (a), biofilm thickness, $L(t)$, (b), substrate concentration in the biofilm, $S(t)$, (c), and active biomass volume fraction, $f(t)$, (d), over 50 days for the zero-dimensional BGM	80
40	Bulk substrate concentration, $S_b(t)$ over .001 days, (a), and .05 days, (b) and substrate concentration in the biofilm, $S(t)$, over .001 days, (c), and .05 days, (d) for the zero-dimensional Rittman's model (dashed line), BAM (solid line), and BGM (dash-dot line)	88
41	Bulk substrate concentration, $S_b(t)$, (a), biofilm thickness, $L(t)$, (b), substrate concentration in the biofilm, $S(t)$, (c), and active biomass volume fraction, $f(t)$, (d), over .001 days for the zero-dimensional Rittman's model (dashed line), BAM (solid line), and BGM (dash-dot line)	88
42	Bulk substrate concentration, $S_b(t)$, (a), biofilm thickness, $L(t)$, (b), substrate concentration in the biofilm, $S(t)$, (c), and active biomass volume fraction, $f(t)$, (d), over 10 days for the zero-dimensional Rittman's model (dashed line), BAM (solid line), and BGM (dash-dot line) . . .	89
43	Bulk substrate concentration, $S_b(t)$, (a), biofilm thickness, $L(t)$, (b), substrate concentration in the biofilm, $S(t)$, (c), and active biomass volume fraction, $f(t)$, (d), over 50 days for the zero-dimensional Rittman's model (dash line), BAM (solid line), and BGM (dash-dot line)	89
44	Bundle of identical capillaries in parallel representing a porous medium	99
45	Bundle of parallel capillaries of different diameters representing a porous medium	101
46	Illustration of the physical basis of the capillaric model of permeability expressed by (4.27)	101

47	Illustration of the physical basis of the capillarie model of permeability expressed by (4.28) and (4.29)	103
48	Bed of identical spherical balls modeling a porous medium	104
49	Biofilm growth in porous media and fluid flow	106
50	A sample porous medium of bulk volume V_{bulk} and height Δz with n , initially uniform, capillaries of diameter D_p	108
51	Experimental normalized permeability, $\hat{k}_e(z, t)$ and porosity, $\hat{\phi}_e(z, t)$, from Cunningham's experimental model, [6]. Porosity is represented by 'x' and the corresponding permeability is represented by 'o'. The solid lines passing through the data points are cubic splines through the data points.	121
52	Experimental normalized permeability, $\hat{k}_e(z, t)$, (o) and porosity, $\hat{\phi}_e(z, t)$, (x) from Cunningham's experimental model, [6]. The computed normalized permeability, $\hat{k}_1(z, t)$, in a bundle of capillary tubes (dashed line) and the computed normalized permeability, $\hat{k}_2(z, t)$, in a bed of spheres (dash-dot line) are shown.	121
53	Substrate concentration, $S_b(z, t)$, in the bulk liquid in the pore channels over .1 days (a), .5 days (b), 1 day (c), and 8 days (d)	123
54	Substrate concentration, $S_b(z, t)$, in the bulk liquid in the pore channels over 20 days	124
55	Substrate concentration, $S(z, t)$, in the biofilm over (a) .1 days, (b) .5 days, (c) 1 day, and (d) 8 days	125
56	Substrate concentration, $S(z, t)$, in the biofilm on the spheres over 20 days	125
57	Active biomass volume fraction, $f(z, t)$, (solid line) and inactive biomass volume fraction, $\bar{f}(z, t)$, (dashed line) over 8 days	127
58	Active biomass volume fraction, $f(z, t)$, (solid line) and inactive biomass volume fraction, $\bar{f}(z, t)$, (dashed line) over 20 days	127
59	Average biofilm thickness on the spheres, $L(z, t)$, over 8 days	129
60	Average biofilm thickness on the spheres, $L(z, t)$, over 20 days	129
61	Average pore volume, $V_L(z, t)$, over 8 days	130
62	Average pore volume, $V_L(z, t)$, over 20 days	131
63	Numerical porosity, $\phi_n(z, t)$, of the porous medium over 20 days	132
64	Numerical permeability, $k_n(z, t)$, of the porous medium over 20 days	133
65	Normalized numerical porosity, $\hat{\phi}_n(z, t)$, (dashed line) and numerical permeability, $\hat{k}_n(z, t)$, (dash-dot line) over 20 days	133
66	Numerical volumetric flow rate, $Q_n(z, t)$, over 8 days	135
67	Numerical volumetric flow rate, $Q_n(z, t)$, over 20 days	135
68	Normalized numerical porosity, $\hat{\phi}_n(z, t)$ (dashed line), normalized experimental porosity, $\hat{\phi}_e(z, t)$ (solid line), normalized numerical permeability, $\hat{k}_n(z, t)$ (dash-dot line), and normalized experimental permeability, $\hat{k}_e(z, t)$ (solid line)	137

69	Experimental (solid line) volumetric flow rate, $Q_e(z, t)$, and numerical (dashed line) volumetric flow rate, $Q_n(z, t)$, over 8 days	139
70	Normalized permeability as a function of normalized experimental porosity. Solid line represents the normalized experimental permeability, dashed line represents the computed normalized permeability, $\hat{k}_c(z, t)$, using (5.15), and dotted line represents the computed normalized permeability, $\hat{k}_c^*(z, t)$, using (5.16)	142
71	Upper three curves represent porosities and the lower three curves represent permeabilities. Solid curves represent experimental data ($\hat{\phi}_e(z, t)$ and $\hat{k}_e(z, t)$). The dotted curves represent the computed normalized numerical porosity ($\hat{\phi}_n(z, t)$) and computed normalized numerical permeability ($\hat{k}_n(z, t)$) using (5.15). The dashed and dash-dot curves represent the computed normalized numerical porosity ($\hat{\phi}_n^*(z, t)$) and computed normalized numerical permeability ($\hat{k}_n^*(z, t)$), respectively, using (5.14).	143
72	Experimental volumetric flow rate, $Q_e(z, t)$, (solid line), numerical volumetric flow rate, $Q_n^*(z, t)$, (dotted line) computed using (5.15), and numerical volumetric flow rate, $Q_n(z, t)$, (dashed line), computed using (5.14)	143
73	Substrate concentration in the bulk liquid, $S_b(z, t)$, at the points z_1^* ($S_{b1}(t)$), z_2^* ($S_{b2}(t)$), and z_3^* ($S_{b3}(t)$) over 20 days. Solid line represents $S_{b1}(t)$, dotted line represents $S_{b2}(t)$ and the dashed line represents $S_{b3}(t)$.	147
74	Steady state (last 18 days) of the substrate concentration, $S_b(z, t)$ in the bulk liquid at z_1^* ($S_{b1}(t)$), z_2^* ($S_{b2}(t)$), and z_3^* ($S_{b3}(t)$). Solid line represents $S_{b1}(t)$, dotted line represents $S_{b2}(t)$ and the dashed line represents $S_{b3}(t)$	147
75	Substrate concentration in the biofilm, $S(z, t)$, at the points z_1^* ($S_1(t)$), z_2^* ($S_2(t)$), and z_3^* ($S_3(t)$) over (a) .001 days (b) .01 days (c) .1 days and (d) 1 day. The solid line represents $S_1(t)$, the dotted line represents $S_2(t)$, and the dashed line represents $S_3(t)$	149
76	Substrate concentration in the biofilm, $S(z, t)$, at the points z_1^* ($S_1(t)$), z_2^* ($S_2(t)$), and z_3^* ($S_3(t)$) over 20 days. The solid line represents $S_1(t)$, the dotted line represents $S_2(t)$ and the dashed line represents $S_3(t)$	150
77	Steady state (last 18 days) of the substrate concentration in the biofilm at the points z_1^* ($S_1(t)$), z_2^* ($S_2(t)$), and z_3^* ($S_3(t)$). The solid line represents $S_1(t)$, the dotted line represents $S_2(t)$ and the dashed line represents $S_3(t)$	151
78	Average active biomass volume fraction, $f(z, t)$, at the points z_1^* ($f_1(t)$), z_2^* ($f_2(t)$), and z_3^* ($f_3(t)$) and the average inactive biomass volume fraction, $\bar{f}(z, t)$, at the points z_1^* ($\bar{f}_1(t)$), z_2^* ($\bar{f}_2(t)$), and z_3^* ($\bar{f}_3(t)$) over 20 days. The solid lines represent $f_1(t)$ and $\bar{f}_1(t)$, the dotted lines represent $f_2(t)$ and $\bar{f}_2(t)$, and the dashed lines represent $f_3(t)$ and $\bar{f}_3(t)$.	153

79	Biofilm thickness, $L(z, t)$, at the points z_1^* ($L_1(t)$), z_2^* ($L_2(t)$), and z_3^* ($L_3(t)$). Solid line represents $L_1(t)$, the dotted line represents $L_2(t)$ and dashed line represents $L_3(t)$ over 20 days.	156
80	Pore volume, $V_L(z, t)$, at the points z_1^* ($V_{L1}(t)$), z_2^* ($V_{L2}(t)$), and z_3^* ($V_{L3}(t)$). Solid line represents $V_{L1}(t)$, dotted line represents $V_{L2}(t)$ and dashed line represents $V_{L3}(t)$ over 20 days.	158
81	Porosity $\phi(z, t)$, at the points z_1^* ($\phi_1(t)$), z_2^* ($\phi_2(t)$), and z_3^* ($\phi_3(t)$). Solid line represents $\phi_1(t)$, dotted line represents $\phi_2(t)$ and dashed line represents $\phi_3(t)$ over 20 days.	160
82	Steady state (last 18 days) of the porosity at the points z_1^* ($\phi_1(t)$), z_2^* ($\phi_2(t)$), and z_3^* ($\phi_3(t)$). Solid line represents $\phi_1(t)$, dotted line represents $\phi_2(t)$ and dashed line represents $\phi_3(t)$	161
83	Permeability $k(z, t)$, at the points z_1^* ($k_1(t)$), z_2^* ($k_2(t)$), and z_3^* ($k_3(t)$). Solid line represents $k_1(t)$, dotted line represents $k_2(t)$ and dashed line represents $k_3(t)$ over 20 days.	162
84	Steady state of the permeability $k(z, t)$, at the points z_1^* ($k_1(t)$), z_2^* ($k_2(t)$), and z_3^* ($k_3(t)$). Solid line represents $k_1(t)$, dotted line represents $k_2(t)$ and dashed line represents $k_3(t)$	163
85	The upper set of curves represents the normalized porosity, $\hat{\phi}(z, t)$, and the lower set of curves represents the normalized permeability, $\hat{k}(z, t)$, at z_1^* , z_2^* , and z_3^* . In the upper set of curves, the solid line represents normalized porosity at z_1^* ($\hat{\phi}_1(t)$), the dotted line represents normalized porosity at z_2^* ($\hat{\phi}_2(t)$), and the dashed line represents the normalized porosity at z_3^* ($\hat{\phi}_3(t)$). In the lower set of curves, the solid line represents the normalized permeability at z_1^* ($\hat{k}_1(t)$), dotted line represents the normalized permeability at z_2^* ($\hat{k}_2(t)$), and the dashed line represents the normalized permeability at z_3^* ($\hat{k}_3(t)$).	164
86	Volumetric flow rate $Q(z, t)$, at the points z_1^* ($Q_1(t)$), z_2^* ($Q_2(t)$), and z_3^* ($Q_3(t)$). Solid line represents $Q_1(t)$, dotted line represents $Q_2(t)$ and dashed line represents $Q_3(t)$ over 20 days.	166
87	Steady state of the volumetric flow rate, $Q(z, t)$, at the points z_1^* ($Q_1(t)$), z_2^* ($Q_2(t)$), and z_3^* ($Q_3(t)$). Solid line represents $Q_1(t)$, dotted line represents $Q_2(t)$ and dashed line represents $Q_3(t)$	167

ABSTRACT

As biofilms intervene in a porous medium, they affect the porosity and permeability, which in turn alters the hydrodynamics. A biofilm growth model is presented which is suitable for microscale simulations of biofilm activity in a porous medium. The model is then used to predict the changing porosity and permeability. The predictions are compared to experimental data and finally these calculated properties are used to simulate flow in a biofilm infested porous medium.

CHAPTER 1

Introduction

The goal of this dissertation is to develop a mathematical model to describe the change in the hydrodynamic properties of a porous medium due to biofilm growth. A one-dimensional mathematical model called the Biofilm Growth Model (BGM) has been developed which describes the growth of biofilm on a surface. The results of the one-dimensional BGM and its zero-dimensional version have been compared. Also the results of the zero-dimensional BGM and the zero-dimensional versions of two existing models called the Biofilm Accumulation Model (BAM) and Rittman's model have been compared. Different model equations relating the porosity and the permeability of a porous medium have been discussed and some of the relations have been compared with the experimental data from [5], [6]. A complete porous media model describing the effect of biofilm growth on porosity, permeability, and hence the flow, has been presented. Finally, the numerical results of the one-dimensional porous media flow model simulations have been presented and these numerical results are compared with the experimental data from [5], [6].

Controlled, artificially grown biofilm in porous media provides significant opportunities for improving the performance of industrial and environmental processes. The petroleum industry, for example, uses biofilm for deliberate plugging of parts of the oil reservoir to enhance oil recovery. A controlled biofilm accumulation in high permeability zones can be used to prevent injection water from reaching the production well. This can be accomplished by injecting cells and nutrients into the oil-bearing formation, [16], [19]. Also, controlling biofilm accumulation is important

to both injection and production well operation in order to avoid unwanted formation plugging near the well bore. The environmental industry likewise uses deliberate plugging of pore channels between spilled contaminants and lakes or rivers to prevent the contamination of these water resources. Subsurface biofilms also offer the potential for biotransformation of organic compounds providing an in situ method (Figure 1) for treating contaminated groundwater supplies, [4], [26]. The mining industry is developing methods for microbially enhanced leaching of metals from ores and recovery of metals from solutions, [11]. An efficient use of biofilm by engineers

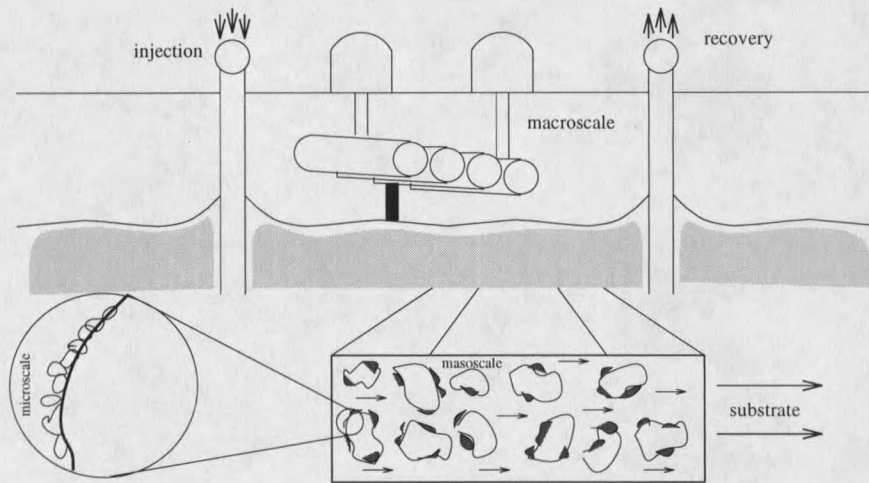


Figure 1: Injection/recovery scheme for enhancing in situ bioremediation of contaminated aquifer. Inset shows the growing biofilm in porous media.

requires an improved understanding of the interrelationship between porous media hydrodynamic properties and the accumulation rate and spatial distribution of the biofilm.

The pressure driven flow between two points in an isotropic homogeneous porous medium depends on the pressure gradient between the two points and the viscosity of the liquid flowing through it as well as the porosity and the permeability of the medium, [2], [7], [20]. If the pressure gradient between the two points and the viscosity of the liquid are assumed to be constant then the porosity and the

permeability dictate the flow rate. If one assumes the presence of an initial thin layer of biofilm on the pore surface and a high concentration of substrate (food for the bacteria) in the liquid flowing through the porous medium then it is reasonable to expect a decrease in the porosity and the permeability of the medium due to the biofilm growth in it. How fast does the biofilm grow? How does the flow rate change? In this work, a mathematical model has been developed that should help in the understanding of these issues.

In order to derive a mathematical model to study the effect of biofilm growth on porous media flow, one must combine the system of flow equations with a system of biofilm growth equations. A one-dimensional mathematical model called the Biofilm Growth Model (BGM) has been developed in Chapter 2 which describes the growth of a biofilm on a surface. The one-dimensional Biofilm Accumulation Model (BAM, [14], originally developed in [25]) and Rittman's model (originally developed in [12]) have also been described in Chapter 2. Based on Rittman's zero-dimensional model, the zero-dimensional versions of BAM and BGM have also been derived. A zero-dimensional model ignores the spatial dependence of the variables, namely the substrate concentration in the biofilm and the volume fraction of the active and inactive bacteria in the biofilm and describes the change in the spatial average value of these variables with respect to time.

A comparison, undertaken in Chapter 3, of the numerical solutions of one-dimensional BGM and zero-dimensional BGM show that (i) the qualitative behavior of the solutions from both the models are very similar and they are also quantitatively close, and (ii) the zero-dimensional model equations are comparatively easy to solve and the computation time is much less than the computation time for the one-dimensional model. The zero-dimensional model lacks some of the features which the one-dimensional model possesses. For example, the substrate concentration or the

active biomass volume fraction at a certain point in the biofilm can not be computed with a zero-dimensional model. However, since we intend to use the biofilm growth model in a porous medium setting, the zero-dimensional BGM is chosen over the one-dimensional BGM. This is because the zero-dimensional model efficiently describes the average change in the substrate concentration and the biofilm thickness which suffices our need. After a comparison of the three zero-dimensional models (BGM, BAM, and Rittman's model), also completed in Chapter 3, the zero-dimensional BGM has been chosen over the other two models primarily because BGM assumes the bulk volume (in the case of a porous medium it is the pore volume) to be a variable as opposed to the other two models (BAM and Rittman's model) in which the bulk volume is assumed to be a constant. This is necessary in order to study the effect of biofilm growth on porosity and hence permeability.

The relation between porosity and permeability of a porous medium has been investigated by many researchers in the past. A collection of experiment-based algebraic relations between porosity and permeability and a list of references can be found in the Chapter 3 of [9]. Some of the relations which are relevant for the models developed in this dissertation are described here in Chapter 4 and the validity of two of such formulas has been checked against the experimental data given in [5], [6]. Finally in Chapter 4, the complete model describing biofilm growth in a porous medium and its effect on porosity and the permeability of the medium is formulated.

The complete model describing the biofilm growth in a homogeneous porous medium and its effect on the one-dimensional incompressible fluid flow through the medium is numerically solved in Chapter 5 and numerical solutions are presented. The model equations are solved for a short bed (5 cm long) of spherical balls and a long bed (60 cm long) of spherical balls. The numerical results for a short bed experiment have been compared with the experimental data from [5], [6]. Lastly, the

change in the variables over time is predicted for a long bed experiment.

CHAPTER 2

Biofilm Models**Introduction**

What follows is the discussion of biofilm growth on a surface. In addition, the derivation of one-dimensional and zero-dimensional mathematical models which describe these physical phenomena is given.

Consider a water filled tank with an initial biofilm thickness on one of its walls. Assume that the substrate (food or nutrient) for the bacteria is dissolved in the water and diffuses into the biofilm. The bacteria in the biofilm will consume the substrate and will multiply. The growth of the biofilm (increase in thickness) depends on the volume fraction of the active biomass, the substrate concentration in the biofilm, the substrate concentration in the bulk liquid in the tank, the rate of the consumption of the substrate by the bacteria, the diffusion rate of the substrate in the biofilm, and possibly other factors. In fact, the growth of the biofilm is a very complicated phenomenon and to produce an accurate mathematical model is not easy. This physical system is shown in Figure 2, where $L(t)$ is the biofilm thickness at time t , $u(L, t)$ is the biomass velocity at the film-water interface and Q is the volumetric flow rate of the influent fluid.

A similar problem has been discussed in [12] and [25] and one-dimensional models have been derived that describe the growth of the thickness of a biofilm with respect to time and space. The model developed in [12] is also called **Rittman's**

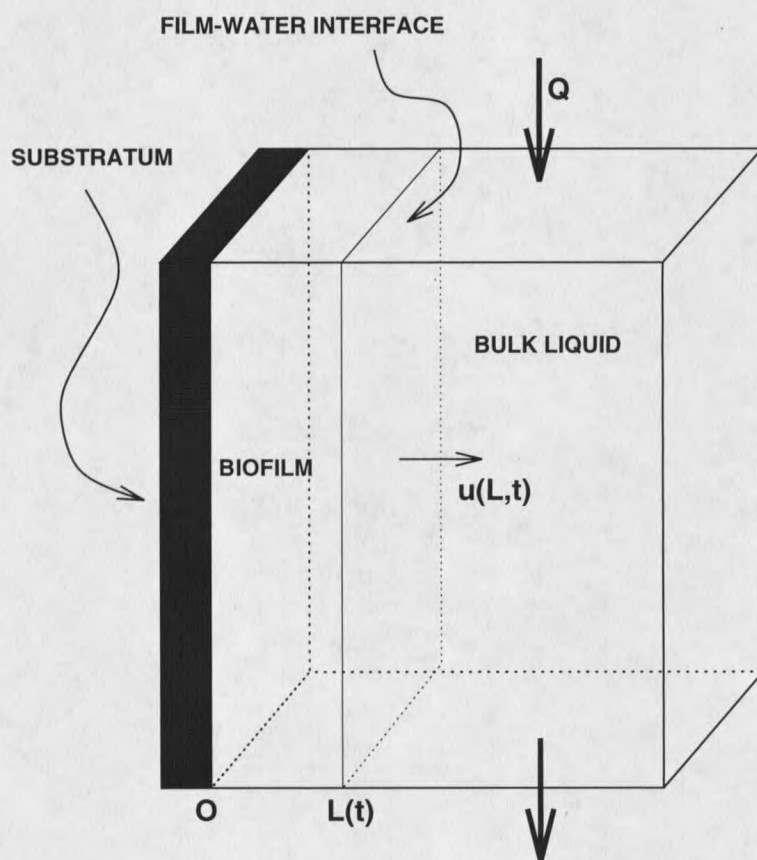


Figure 2: Biofilm on a surface

Model. The Center for Biofilm Engineering at Montana State University, has developed a computer simulator called the **Biofilm Accumulation Model, (BAM)**, [14] which studies the growth of biofilm on a flat surface. The model equations are based on [25]. Both of these models assume the volume of the bulk liquid is constant. Also some of the terms in the model equations are not consistent with the underlying assumptions. Hence a new model called the **Biofilm Growth Model (BGM)** is developed here which considers the volume of the bulk liquid to be a time-dependent function instead of a constant. The equations described in these models cannot be used directly in a problem where biofilm grows in a porous media because of the simplified assumptions of these models and the complicated geometry of the pore surface, however the idea of the zero-dimensional model discussed in [12] is very useful here. In both Rittman's model and BAM, different types of bacteria are consuming different types of substrates and are growing simultaneously. But, for now, in order to keep the notation clean and the problem simple and explainable, we shall restrict ourselves to only one bacteria consuming only one substrate.

Rittman's Model

One-dimensional Model

In this model, originally proposed in [12], the microbial interactions and diffusion phenomena are described by two sets of mathematical equations. The first set is called diffusional equations, the other one transport equations. They are derived from basic mass balances. The following *a priori* assumptions have been made to develop this model:

- The biofilm is homogeneous and can be treated as a continuum.
- Changes occur only in the direction normal to the biofilm surface.

- There is a laminar diffusional sublayer of constant thickness in the bulk liquid.
- The biofilm is composed entirely of active or inactive biomass.

This model predicts four time-dependent functions, two of which depend on the spatial variable y as well. These functions and their fundamental units of length (L) and substrate mass (M_s) are given in Table 1.

Variables	Physical quantity	Units
$L(t)$	biofilm thickness	L
$S_b(t)$	bulk substrate concentration	$M_s L^{-3}$
$S(y, t)$	substrate concentration in the biofilm	$M_s L^{-3}$
$f(y, t)$	volume fraction of active biomass in the biofilm	dimensionless

Table 1: Unknown dependent variables and their fundamental units in Rittman's one-dimensional model

Other variables and the parameters used in the development of this model and their fundamental units of length (L), time (T), substrate mass (M_s), and biomass (M_x), are given in Table 2.

A visualization of the physical system to be modeled is given in Figure 3 where σ is the surface area of the film-water interface.

Diffusional Equations The mass balance equation for the total substrate in the bulk liquid, $V_L S_b$, has the form

$$V_L \frac{d}{dt}(S_b(t)) = Q(S_0 - S_b(t)) - \sigma J(t), \quad (2.1)$$

where V_L is the volume (L^3), Q represents the bulk liquid flow rate ($L^3 T^{-1}$), σ is the surface area of the film-water interface (L^2), S_0 refers to the influent substrate concentration ($M_s L^{-3}$) and $J(t)$ refers to the substrate flux through the laminar diffusional sublayer ($M_s L^{-2} T^{-1}$). V_L, Q, σ and S_0 are assumed constant. According

Parameters	Physical quantity	Units
V_L	volume of the bulk liquid	L^3
Q	volumetric flow rate of the bulk liquid	L^3T^{-1}
S_0	substrate concentration in the influent fluid	M_sL^{-3}
σ	area of the film-water interface	L^2
D	diffusivity coefficient of the substrate through the laminar diffusional sublayer	L^2T^{-1}
L_l	thickness of laminar diffusional sublayer	L
d	diffusivity coefficient of the substrate inside the biofilm	L^2T^{-1}
V_r	maximum specific growth rate	$M_sM_x^{-1}T^{-1}$
K	Monod constant	M_sL^{-3}
ρ	biomass density	M_xL^{-3}
b	inactivation coefficient of bacteria	T^{-1}
Y	yield coefficient	$M_xM_s^{-1}$
G_s	global shear stress coefficient	T
B'	average shear stress coefficient	T^{-1}
f_d	biodegradable fraction of the biomass	dimensionless
Variables	Physical quantity	Units
$J(t)$	influx rate of the substrate into the biofilm	$M_sL^{-2}T^{-1}$
$u(y, t)$	velocity of the biomass particle at (y, t)	LT^{-1}
$G(y, t)$	active biomass quantity in the interval $[0, y]$	M_xL^{-2}
$c(y, t)$	net growth of active biomass	$M_xL^{-3}T^{-1}$
$R(y, t)$	reaction rate	$M_sL^{-3}T^{-1}$
$b'(y)$	shear function along y-axis	T^{-1}
$f_0(t)$	volume fraction at the substratum	dimensionless
$\bar{G}(y, t)$	inactive biomass quantity in the interval $[0, y]$	M_xL^{-2}
$\bar{f}(y, t)$	volume fraction of inactive biomass in the biofilm	dimensionless
$\bar{c}(y, t)$	net growth of inactive biomass	$M_xL^{-3}T^{-1}$
$B(y, t)$	total biomass amount	M_xL^{-2}

Table 2: Parameters and the variables used in Rittman's model and their fundamental units

